

Optimal Stroke Learning with Policy Gradient Approach for Robotic Table Tennis*

Yapeng Gao¹, Jonas Tebbe¹ and Andreas Zell¹

Abstract—Learning to play table tennis is a challenging task for robots, due to the variety of the strokes required. Current advances in deep Reinforcement Learning (RL) have shown potential in learning the optimal strokes. However, the large amount of exploration still limits the applicability when utilizing RL in real scenarios. In this paper, we first propose a realistic simulation environment where several models are built for the ball’s dynamics and the robot’s kinematics. Instead of training an end-to-end RL model, we decompose it into two stages: the ball’s hitting state prediction and consequently learning the racket strokes from it. A novel policy gradient approach with TD3 backbone is proposed for the second stage. In the experiments, we show that the proposed approach significantly outperforms the existing RL methods in simulation. To cross the domain from simulation to reality, we develop an efficient retraining method and test in three real scenarios with a success rate of 98%.

I. INTRODUCTION

Reinforcement Learning (RL) has recently achieved a variety of successes, especially in autonomous driving [1], gaming [2], [3] and robotics manipulation [4], [5]. In RL one studies an agent in its surroundings. Based on the observed state, the agent can take actions in the environment and subsequently perceive a reward that indicates whether these actions were performed well or not. This is defined as a Markov Decision Process (MDP). The goal of RL is to maximize the expected value of the cumulative reward in one episode. However, a large amount of exploration is usually required to formulate a near-optimal policy of actions.

To address this problem, one common way is creating a simulation environment to train a model and then transfer it to reality. [6] randomly simulated dynamics parameters (link mass, joint damping, puck friction, etc.) for a 7-DOF fetch robot arm and considered them as a part of the current state. Meanwhile, Gaussian noise was applied on each joint position, velocity, and the gripper position. Based on DDPG [7], this dynamics randomization method can cross the reality gap and perform equally well on a real robot. With a similar idea, [8] trained dexterous in-hand manipulation policies entirely in simulation, by randomizing many of the physical properties, such as the friction coefficients and the object’s appearance. A scaled PPO [9] algorithm was developed for training. Although dynamics randomization has shown some success, it requires a lot of time and hardware to be able to converge during training. For robotic table tennis

we are seeking an efficient and effective approach to learn the optimal stroke. Another problem caused by the existing RL methods, like TRPO [10], PPO, DDPG, TD3 [11], or SAC [12] is the fuzzy one-dimensional reward that cannot precisely express the interaction with the environment for multi-dimensional actions.

Inspired by the aforementioned methods, in this paper we propose a novel approach for optimal stroke learning in robotic table tennis. Two learning steps, including the training in simulation and the retraining in reality, can be completed in around 4 hours for various spin balls. The main contributions of this paper are as follows:

- We design a realistic simulation in combination with the Gazebo simulator, Robot Operating System (ROS), OpenAI Gym [13] and the RL library Spinning Up. The robot and table tennis ball are controlled by the Gazebo plugin. Different parts can communicate with each other via ROS topics.
- We decompose the learning strategy into two stages: the ball hitting state prediction and the optimal stroke learning, on which we mainly focus in this work. Based on the controllable and applicable actions in our robot, a multi-dimensional reward function and Q -value model are proposed.
- The comparison with other RL methods is performed using an evaluation dataset of 1000 balls in simulation. An efficient retraining approach is proposed to close the sim-to-real gap. The testing experiments in reality show that the robot can successfully return the ball to the desired target with the error of around 24.9 cm and a success rate of 98% in three different scenarios.

II. RELATED WORK

A. Simulation for robotic table tennis

In simulated environments, the robot can freely explore various actions and alleviate the safety concerns during the training steps. Meanwhile, simulation can provide a fair and deterministic environment for comparing the performance of different approaches. In [14], PyBullet was used to create the physical entities. In order to learn from demonstrations, they connected a virtual reality (VR) setup with the simulator and captured the human actions with a instrumented racket. In [15], a simple simulation was built on top of MATLAB. To make use of robotic drivers and devices, [16] implemented a quadrotor model in the Gazebo simulator, which can be easily combined with ROS. [17] developed a hybrid simulation and real training for muscular robots. They

*Thanks to the Vector Stiftung and KUKA for support

¹Yapeng Gao, Jonas Tebbe and Andreas Zell are with the Cognitive Systems group, Computer Science Department, University of Tuebingen, 72076 Tuebingen, Germany [yapeng.gao, jonas.tebbe, andreas.zell]@uni-tuebingen.de

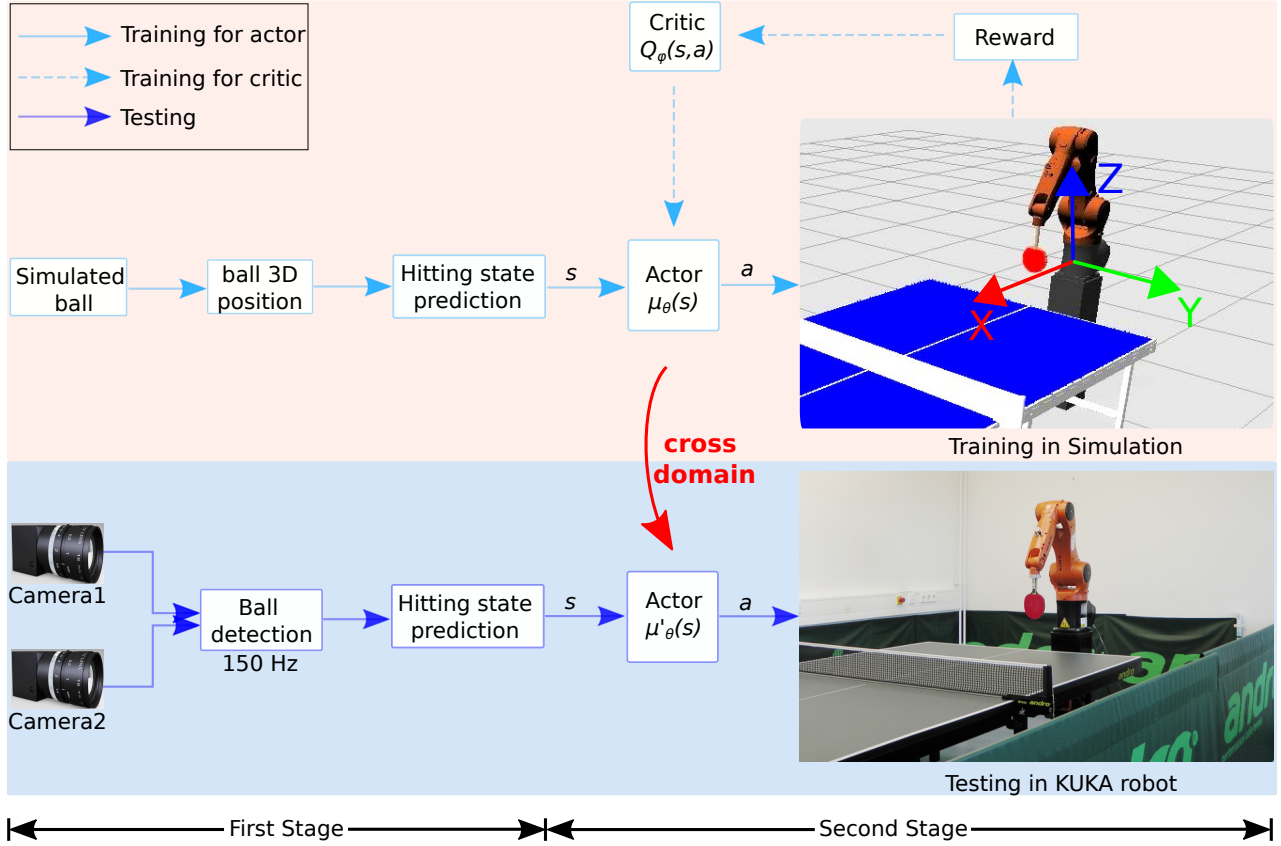


Fig. 1. The whole framework for training and testing. The first stage is used for predicting the ball's state s at the hitting point at a frequency of 150 Hz. In this paper we focus on the second stage where a optimal stoke can be learnt based on a novel RL algorithm. The upper part is performed in simulation. A proposed RL model is trained within 10,000 episodes. To cross the “reality gap”, we retrain the model in an efficient way. The world coordinate system is identical to the robot's, which is shown in simulation image.

duplicated the incoming ball's state from reality to simulation and then simulated the impact with the racket to estimate the ball's landing position. However, these simulations are not realistic enough, which results in more effort on transferring from simulation to reality. In addition, some of them are not compatible with the existing RL libraries that include some advanced RL algorithms. Therefore, we designed a realistic simulation in combination with the Gazebo, ROS, OpenAI Gym and Spinning Up. The ball's dynamics is determined based on [18], [19].

B. Reinforcement learning in robotic table tennis

Recently, deep RL has attracted a lot of interest by researchers in robotic table tennis. [20] developed an end-to-end algorithm to directly learn to control a simulated table tennis robot in joint space. They took the joint position trajectories and ball locations as input and trained a multi-modal model-free policy to learn the velocities for each joint. In [17], a hybrid simulation and reality (HYSR) system was introduced to train a muscular table tennis robot in joint space. They leveraged PPO as the backbone. However, this end-to-end approach is not efficient for training (need about 14 hours to train for a set of similar ball trajectories). [14] incorporated the stroke learning into a hierarchical control system that includes the inverse landing model, analytic

racket controller, forward racket mode and forward landing model. Each model was trained separately to make the learning process easier and more efficient. [21] adopted a two-stage approach for stroke learning. In the first stage, the ball's hitting states (position and velocity) were determined by an extended Kalman filter (EKF) based predictor. Then, these states were fed into the DDPG as inputs, the outputs were the racket's velocity. Instead the DDPG, [22] utilized an accelerated parametrized-reward gradients approach to learn the racket's velocity from the predicted hitting states. This was trained by 200 human demonstrations.

III. METHODOLOGY

To learn the optimal stroke efficiently and hit the ball to the desired target on the table successfully, we propose a novel framework, as shown in Fig. 1. A realistic simulation environment is developed for robot learning and for comparison with other advanced RL algorithms. The ball's hitting state (position, velocity, spin) can be predicted by the approaches in our previous works [19], [23]. In the second stage, a novel approach is employed to learn the optimal stroke in simulation, which is conjugated with ROS and OpenAI libraries

A. Simulation

A challenge for deep RL is how to safely interact with the environment. In robotic table tennis, it is difficult to explore every possibility since unexpected collisions would destroy the mechanical robot parts. In addition, the robot has to interact with the environment for a large number of steps to learn a high level policy. To address these problems, we develop a realistic simulation that can provide a convenient scenario for optimal stroke learning as well as a comparison of different algorithms. The pose and velocity of the racket is controlled by the simulator. The dynamics models of the ball are as follows:

1) *Flying Ball Model*: Except for the gravitational force F_g , a flying ball is usually influenced by the Magnus force F_m and the air drag F_d [24]. As shown in Fig. 2, F_m is perpendicular to the spin axis and the flight direction. F_d is opposite to the flight direction.

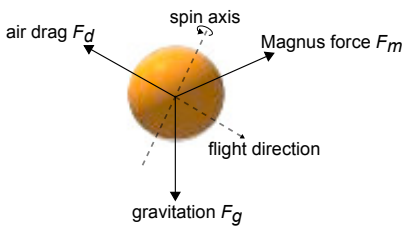


Fig. 2. Force analysis in a flying ball. A sphere shell of radius r_1 and mass m , with centered spherical cavity of radius r_2 , is created as the simulated ball in Gazebo.

These forces can be computed by the following formulas:

$$F_g = (0, 0, -mg)^T \quad (1)$$

$$F_d = -\frac{1}{2} C_D \rho_a A \|v\| v \quad (2)$$

$$F_m = \frac{1}{2} C_M \rho_a A r_1 (\omega \times v) \quad (3)$$

where the constants are determined in our previous work [23] including the ball's mass $m = 2.7\text{g}$, the gravitational constant $g = 9.81\text{m/s}^2$, the drag coefficient $C_D = 0.4$, the air's density $\rho_a = 1.29\text{kg/m}^3$, the lift coefficient $C_M = 0.6$, the ball's radius $r_1 = 20\text{mm}$, the cavity radius $r_2 = 19.6\text{mm}$, and the ball's cross-section $A = r_1^2 \pi$. ω and v are the linear and angular velocity. Given the ball's trajectory in reality, ω and v can be derived for the hitting state prediction by the algorithm in [19], [23]. To simulate the accurate dynamics of the ball, we also need the inertia value I calculated by

$$I = \frac{2}{5} m \left(\frac{r_1^5 - r_2^5}{r_1^3 - r_2^3} \right) \quad (4)$$

2) *Bounce Model*: In reality, the physical contact between two objects is a very complex thing. To approximate the contact forces between the ball and the table (or the racket), we adopt the Open Dynamics Engine (ODE) which is a popular rigid body dynamics library for robotics. It is already built in the Gazebo simulator. To represent the elastic and frictional impacts on the ball, we compute the restitution coefficient κ_R and the friction coefficient μ similar to [25].

The restitution coefficient κ_R is defined as the ratio of the energy before and after a collision, for example, when the ball bounces off the table. Approximately, it can be solved by a free fall of the ball as follows:

$$\kappa_R^t = \frac{v_2^t - v_1^b}{v_1^b - v_1^t} = \frac{-v_2^b}{v_1^b} = \frac{-\sqrt{2 \cdot g \cdot h_2}}{-\sqrt{2 \cdot g \cdot h_1}} = \sqrt{\frac{h_2}{h_1}} \quad (5)$$

where v_1^b and v_1^t are the velocity of the ball and table before impact, v_2^b and v_2^t are after. h_1 and h_2 are the corresponding heights when the ball is not moving. Here the table velocity $v^t = 0$.

The friction coefficient μ is obtained by the setup in Fig. 3. Three balls are arranged together in form of a triangle frame. We first put them on the table, and lift the table until it begins to slide. According to the horizontal angle change θ of the table, we can get the friction coefficient μ^t between the table and the ball by

$$\mu^t = \frac{3mg \cdot \sin \theta}{3mg \cdot \cos \theta} = \tan \theta \quad (6)$$



Fig. 3. Setup for measuring the friction coefficient μ .

We use the same methods to compute the racket's restitution coefficient κ_R^r and friction coefficient μ^r . The resulting parameter values are in the Table I. Additional required parameters μ_2 and *slip* are defined as the friction coefficient in second ODE friction pyramid direction and the coefficients of force-dependent-slip (FDS), respectively. They are manually adjusted to fit the reality.

TABLE I
COLLISION PARAMETER VALUES WHEN THE BALL IMPACTS ON THE
TABLE AND RACKET.

	κ_R	μ	μ_2	<i>slip</i>
Table	0.97	0.05	0.025	0.01
Racket	0.9	1.0	0.025	0.01

B. Algorithm

With regard to the different types of inputs, there are usually two ways available when using deep RL algorithms in robotic table tennis. The first are one-stage algorithms, which take the ball's state of every step as inputs and learn the racket's pose in an end-to-end way. Others are two-stage algorithms, which first predict the ball's hitting state and then consider it as inputs. The latter one can significantly accelerate the training step and can handle different spin balls. In this paper we adopt the second way to learn the optimal stroke of the racket based on the state prediction of the ball at the hitting point.

Since there is only a single state vector as input in the second stage, we then parameterize the stroke learning as a bandit problem, where actions have no influence on next states and consequently there are not any delayed rewards in one episode. It is a simple version of an Markov Decision Process (MDP), with

$$M = (S, A, R) \quad (7)$$

where S is the set of the observed 11-D states s including the ball 3D position p^b , 3D linear velocity v^b , 3D angular velocity ω^b at the hitting time, and the desired 2D landing target p^{tar} on the table. A is the set of 3D actions a that can be performed on the robot. Due to the restriction of the current mechanical structure and the control system, we can not operate the robot as flexibly as a human can move. Therefore, we only learn to change the robot's linear velocity v_x^r along the x -axis and the orientation angles (β^r, γ^r) around the y and z axes. The racket's target position is the same as the predicted hitting position of the ball. R is a set of the immediate rewards r .

We utilize a policy $\mu_\theta(s)$ as the actor network which can output the actions a with respect to the current state s as shown in Fig. 4 left. To evaluate the actions, a critic network $Q_\phi(s, a)$ is used, which takes as input both the states and actions and outputs a Q -value, as shown in Fig. 4 right. θ and ϕ are the neural network weights. The goal is to learn a deterministic policy $\mu_\theta(s)$, which provides an action that maximizes $Q_\phi(s, a)$. According to the DDPG algorithm, the critic and the actor can be updated, respectively, by minimizing the losses:

$$\mathcal{L}(\phi, \mathcal{D}) = \mathbb{E}_{(s, a, r) \sim \mathcal{D}} [(Q_\phi(s, a) - r)^2] \quad (8)$$

$$\mathcal{L}(\theta, \mathcal{D}) = -\mathbb{E}_{s \sim \mathcal{D}} [Q_\phi(s, \mu_\theta(s))] \quad (9)$$

where \mathcal{D} is the experience replay buffer for storing s, a, r . The reward r is the feedback from the environment, which we will discuss in more detail later.

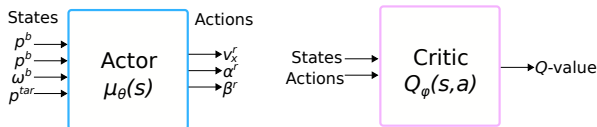


Fig. 4. Classic Actor-Critic algorithms. Instead a 1D Q-value, we propose a 3D Q-value to train the corresponding 3D actions.

To accelerate the training step and boost the resulting performance, we apply the following changes to the classic actor-critic algorithms during training:

1) *Exploration*: For continuous action spaces several exploration policies are used in the deterministic environments. The *random* strategy selects the actions randomly from a Gaussian distribution, the *epsilon-greedy* strategy takes the random actions occasionally with probability ϵ and uses the output from the current actor $\mu_\theta(s)$ with probability $1-\epsilon$. In [26] an additional stochastic policy is deployed to learn

how to explore. We noticed that the actor $\mu_\theta(s)$ did not give the action with the maximum Q -value in the earlier training step because of the large loss error. Therefore, we generate the actions a by

$$a = \operatorname{argmax}_{\mu_\theta(s) + \mathcal{N}} Q_\phi(s, \mu_\theta(s) + \mathcal{N}) \quad (10)$$

where \mathcal{N} is a Gaussian noise.

2) *Reward shaping*: In [21], they develop a reward function that depends on the ball's height h^b across the net and the real landing position p^{real} on the table when the ball is returned. A coefficient value is used to balance the h^b and p^{real} . Then a tricky part is how to select this value. To address this problem, we separate the reward into three vector components: r_h for the height, r_x and r_y for the landing position. Each reward function then is normalized to [0,1] by the following equations:

$$r_x = e^{-|p_x^{real} - p_x^{tar}|} \quad (11)$$

$$r_y = e^{-|p_y^{real} - p_y^{tar}|} \quad (12)$$

$$r_h = e^{-|h^b - 0.173|} \quad (13)$$

$$r = [r_x, r_y, r_h] \quad \text{if success else } \vec{0} \quad (14)$$

where p_x and p_y are the landing position in meters along the x and y axes. 0.173 is the net height in meters. e is the natural exponential operation. When a ball is successfully returned to the opposing table, *success* is set to true.

3) *3D Q-value*: Normally, the Q -value is a 1D vector which is expected to be maximized. To make use of the above rewards, we replace the last layer in the critic network from 1D to 3D. This results in a 3D Q -value $[Q_x, Q_y, Q_h]$, which can precisely indicate the quality of the actions.

In addition, for the actor-critic model we adopt TD3 as the backbone. The critic is changed to:

$$Q_\phi(s, a) = \begin{cases} Q_{\phi_1}(s, a), & \text{if } \|Q_{\phi_1}(s, a)\| < \|Q_{\phi_2}(s, a)\| \\ Q_{\phi_2}(s, a), & \text{otherwise} \end{cases} \quad (15)$$

The whole training process is depicted in Algorithm 1.

IV. EXPERIMENTS

A. Training and Testing

With random serves in simulation, we can obtain a number of unique states s for each episode. To generalize the trained model, these serves are sampled from a wide range of values. Meanwhile, 1,000 serves are collected for a fair evaluation. To bridge the "reality gap", we first apply some Gaussian noise to each ball's 3D position in simulation. Instead of using the true states of the ball in simulation, we then predict the states at the hitting point with the methods in [19], [23]. The predicted hitting position is actually what the simulated racket should move to. This can replicate the real situation and make the trained model more realistic for the real world. The final state range is shown in Table II, which includes the desired landing target (p_x^{tar}, p_y^{tar}) , the ball position (p_x^b, p_y^b, p_z^b) , linear velocity (v_x^b, v_y^b, v_z^b) , and angular velocity $(\omega_x^b, \omega_y^b, \omega_z^b)$ at the hitting point. These states are

Algorithm 1 Policy Gradient Training with TD3 backbone

Input: Initial actor weights θ , critic weights ϕ_1, ϕ_2 , replay buffer \mathcal{D} , number of episodes λ , Gaussian noise $\mathcal{N}(0, 0.1)$

Output: Optimal policy $\mu_\theta^*(s)$

- 1: **for** $n=1$ to λ **do**
- 2: Observe the state s and generate the action a by
- 3: $\text{argmax}_{\mu_\theta(s)+\mathcal{N}} Q_\phi(s, \mu_\theta(s) + \mathcal{N})$
- 4: Apply a in the environment and get the reward r
- 5: Store (s, a, r) in the replay buffer \mathcal{D}
- 6: Reset the environment
- 7: **if** it is time to update **then**
- 8: Sample a random minibatch \mathcal{B} from \mathcal{D}
- 9: **for** $i=1,2$ **do**
- 10: Update the critic by minimizing the loss:
- 11: $\mathcal{L}(\phi_i, \mathcal{B}) = \mathbb{E}_{(s, a, r) \sim \mathcal{B}} [(Q_{\phi_i}(s, a) - r)^2]$
- 12: **end for**
- 13: **if** it is time to update actor **then**
- 14: Update the actor by minimizing the loss:
- 15: $\mathcal{L}(\theta, \mathcal{B}) = -\mathbb{E}_{s \sim \mathcal{B}} [Q_\phi(s, \mu_\theta(s))]$
- 16: where $Q_\phi(s, \mu_\theta(s))$ is from Eq. 15:
- 17: **end if**
- 18: **end if**
- 19: **end for**

subsequently normalized as inputs for training. The p_x^b is fixed to form a virtual hitting plane in the first stage.

By considering the robot's mechanical setup, we restrict the robot's linear velocity v_x^r in a range from 0m/s to 2m/s. The orientation angles β^r, γ^r are from -50° to 50° . The third angle α^r around the x -axis is calculated by

$$\alpha^r = k \cdot \frac{p_y^b}{0.5 \cdot w^t} \quad (16)$$

where w^t is the table width, k is a coefficient. In this way, the robot will generate a human-like stroke. In principle, the angle α^r will not influence the impact with the ball.

In Equation 10, The added action noise \mathcal{N} for exploration is a mean-zero Gaussian distribution with a standard deviation of 0.1. The replay buffer \mathcal{D} has a size of 5,000. The number of training episodes λ is 10,000. Other hyperparameters used for actor-critic are given in Table III. The output actions from the actor are scaled to the valid range and then applied to the simulation. These hyperparameters are tuned manually in order to achieve the best performance.

Meanwhile, 1000 episodes are performed after each epoch for testing. The resulting rewards and the corresponding 3D Q -value are plotted in Fig. 5. We can observe that the testing rewards begin to reach the steady levels from the 20th epoch, although the Q -values have not converged to the maximums.

TABLE II

STATE RANGE AT THE HITTING POINT FOR TRAINING AND EVALUATION.

	training	evaluation
p_x^{tar}		2.55m
p_y^{tar}		0.0m
p_x^b		0.675m
p_y^b	[-0.60m, 0.63m]	[-0.68m, 0.68m]
p_z^b	[-0.01m, 0.34m]	[-0.01m, 0.34m]
v_x^b	[-6.00m/s, -1.35m/s]	[-5.94m/s, -2.52m/s]
v_y^b	[-1.95m/s, 2.16m/s]	[-1.29m/s, 2.02m/s]
v_z^b	[-3.47m/s, 3.15m/s]	[-3.40m/s, 2.60m/s]
ω_x^b	[-127.67rad/s, 110.88rad/s]	[-95.08rad/s, 111.53rad/s]
ω_y^b	[-299.99rad/s, 299.81rad/s]	[-299.62rad/s, 299.73rad/s]
ω_z^b	[-193.81rad/s, 189.65rad/s]	[-189.05rad/s, 189.47rad/s]
Episodes λ	10000	1000

TABLE III

HYPERPARAMETERS FOR TRAINING IN SIMULATION AND RETRAINING IN REALITY.

	Actor/Critic	
	Training	Retraining
batch size	512	50
epochs	100	-
episodes per epoch	100	20
learning rate	1e-4	5e-5
optimizer	Adam	
layers	[256, 256, 3]	
activation	relu	
output activation	tanh/linear	

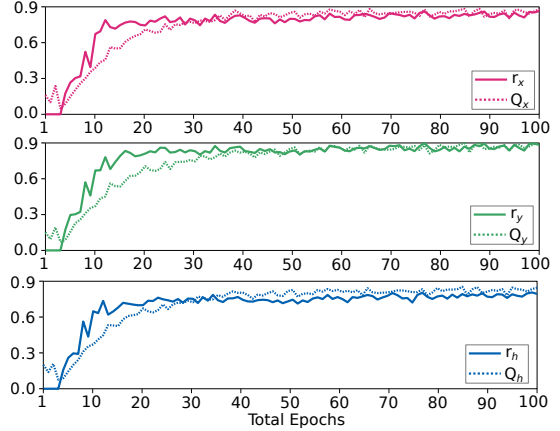


Fig. 5. The testing rewards $[r_x, r_y, r_h]$ and the 3D Q -value $[Q_x, Q_y, Q_h]$ in simulation.

B. Evaluation

A usual metric for the evaluation is the distance error between the real and the desired landing position [14], [17], [21]. However, this metric can not reflect a failed return, for example, if the landing position is not on the table, it will be difficult to calculate the distance error. Therefore, here we

introduce a new metric: distance error ϵ_d computed by:

$$r_d = e^{-||p^{real} - p^{tar}||_2} \quad \text{if success else 0} \quad (17)$$

$$\epsilon_d = -\ln \left(\frac{1}{\lambda} \sum_{n=1}^{\lambda} r_d^n \right) \quad (18)$$

where the r_d^n is the reward for the landing distance error of the n^{th} ball. It is equal to 0 when the ball fails to land on the opposite table. The number of episodes λ is equal to 1000 for evaluation. The second metric ϵ_h , for the ball flying height error across the net, is calculated in the same way. The third metric is the success rate of returning to the opposite table. To give a fair evaluation, we adopt 1000 balls resulting in a large range for the states (see Table II right).

Since the existing RL algorithms are only allowed to use a 1D Q -value, we then create a 1D reward function similar to [21] by

$$r_{eval} = e^{-k(||p^{real} - p^{tar}|| - |h^b - 0.173|)} \quad (19)$$

where k is a scalar coefficient, which is set to 0.5 in this paper. This new reward function is only adopted to train the existing RL algorithms including TRPO, PPO, SAC, DDPG, and TD3. As a result of the different reward functions used for evaluation, we compute the distance error ϵ_d , the height error ϵ_h and the success rate, respectively, which are shown in Table IV. The unit of these errors is converted from meters to centimeters for better visualization. The proposed approach, argmax exploration plus 3D Q -value together with TD3 backbone, achieves better performance than the DDPG backbone. Other three approaches, TRPO, PPO, and SAC, learn the optical stroke using a stochastic policy, which leads to much higher errors and lower success rate.

TABLE IV
EVALUATION FOR DIFFERENT ALGORITHMS.

Algorithms	ϵ_d	ϵ_h	success rate
TRPO	47.0cm	31.0cm	84.8%
PPO	44.2cm	30.8cm	87.1%
SAC	43.5cm	29.0cm	89.2%
DDPG	25.6cm	22.1cm	95.6%
DDPG+argmax	23.0cm	22.3cm	97.4%
DDPG+argmax+3D Q-value	21.3cm	21.7cm	97.9%
TD3	25.2cm	22.3cm	97.2%
TD3+argmax	22.2cm	21.2cm	97.7%
TD3+argmax+3D Q-value	20.3cm	21.2cm	98.5%

C. Retraining in reality

Although we have built a high-fidelity simulation by manually measuring the coefficients and applying random noise on the ball, the real robot has much more dynamic and complicated factors that can not be accurately measured and included. To find the best hyper-parameters for retraining, we first change the racket's restitution coefficient κ_R^r and friction coefficient μ^r in simulation. In this way, we can replicate the situation between two different rackets in reality. Based on the pretrained actor-critic model, we then retrain the model in the new simulation with various batch sizes, episodes per

epoch, and learning rates. The best hyper-parameters found in simulation are shown in Table III right.

A ball throwing machine, TTmatic 404A, is utilized to provide a range of balls with sidespin, topspin, and backspin. At the moment our robot can only handle sidespin and topspin, as the backspin ball causes too high acceleration in a robot joint. This could be solved in the future. The Reflexxes motion library [27] is used for robot trajectory planning in Cartesian space. Each epoch includes both sidespin and topspin balls during retraining. The state range for retraining and testing at the hitting point is shown in Table V. Here, the model is retrained with 20 epochs to ensure it reaches convergence. The hitting position p_x^b along the x axis is fixed to 0.675m. The resulting retraining process, including the landing distance error ϵ_d and the height error ϵ_h , is plotted in Fig. 6.

TABLE V
STATE RANGE AT THE HITTING POINT FOR RETRAINING AND TESTING.

	retraining/testing in machine	testing with human
p_y^b	[-0.55m, 0.64m]	[-0.65m, 0.43m]
p_z^b	[0.085m, 0.34m]	[0.06m, 0.033m]
v_x^b	[-5.20m/s, -3.5m/s]	[-5.6m/s, -2.9m/s]
v_y^b	[-1.05m/s, 2.35m/s]	[-2.38m/s, 1.25m/s]
v_z^b	[-0.78m/s, 3.92m/s]	[-0.4m/s, 2.48m/s]
ω_x^b	[-32.94rad/s, 52.68rad/s]	[-33.00rad/s, 78.48rad/s]
ω_y^b	[-210.52rad/s, 5.33rad/s]	[-182.72rad/s, -55.28rad/s]
ω_z^b	[-157.65rad/s, 34.51rad/s]	[-66.68rad/s, 52.62rad/s]

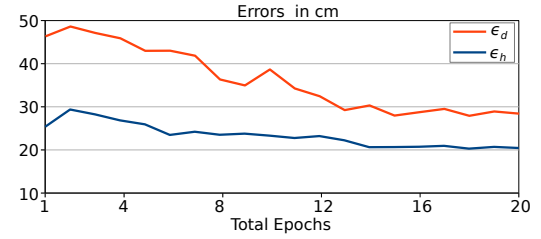


Fig. 6. Retraining process using the ball throwing machine.

D. Testing in reality

To perform a complete test, we conduct the experiments in three scenarios where the complexity rises gradually. First a human player (Player1) serves the ball with different starting positions at the front of the table. In this way, the hitting position can be fully covered along the y -axis. The second player with senior skills (Player2) then plays a long game rally to test the continuous performance of the robot. The state range for these two scenarios is shown in the third column of the Table V. Finally, we use the ball throwing machine (Machine) to generate different balls with various spins and speeds. It is difficult to fairly compare our performance with other work since the scenarios, like the robot, racket, ball state, and human player, are totally different as well as the evaluation metrics. We then give the Table VI by directly using the data in [28], [29] or by manually computing for [17], [22].

TABLE VI
TESTING IN REALITY.

Scenarios	episodes	ϵ_d	ϵ_h	success rate
Büchler et al. [17]	107	76.9cm	-	75%
Mülling et al. [28]	30	46.0cm	-	97%
Kyohei et al. [29]	100	22.5cm	-	99%
Jonas et al. [22]	300	24.2cm	-	93.6%
Player1	40	20.3cm	22.2cm	
Player2	40	25.6cm	23.5cm	98%
Machine	40	28.8cm	20.2cm	

The average ϵ_d and ϵ_h for our three scenarios are 24.9 cm and 21.9 cm, with a standard deviation of 9.0 cm and 4.6 cm, respectively. Playing performance including some failure cases can be found at <https://youtu.be/SNnqtGLmX4Y>.

V. CONCLUSIONS AND FUTURE WORK

In this paper, we first designed a realistic simulation for a table tennis robot. To learn the optimal stroke movement for the robot, we proposed a new policy gradient approach with TD3 backbone. Different algorithms were fairly evaluated in simulation using 1000 balls with a large range of spins and speeds. To cross the domain from simulation to reality, a retraining approach was proposed for the original racket and another coefficient-unknown racket. The testing results in three complicated scenarios with a success rate of 98%.

However, the robot will fail if the incoming ball is too high or too slow, since the target can not be reached at a fast enough speed. Also, the robot will not have sufficient reaction time if the ball is too fast (e.g. 10m/s). In the future we plan to optimize the Reflexxes motion libraries to produce a more applicable trajectory for each spin ball. Instead of constraining the hitting position p_x^b along the x-axis, we can try to parameterize it as one action that needs to be learned.

REFERENCES

- [1] A. Kendall, J. Hawke, D. Janz, P. Mazur, D. Reda, J.-M. Allen, V.-D. Lam, A. Bewley, and A. Shah, "Learning to drive in a day," in *2019 International Conference on Robotics and Automation (ICRA)*. IEEE, 2019, pp. 8248–8254.
- [2] D. Silver, J. Schrittwieser, K. Simonyan, I. Antonoglou, A. Huang, A. Guez, T. Hubert, L. Baker, M. Lai, A. Bolton et al., "Mastering the game of go without human knowledge," *nature*, vol. 550, no. 7676, pp. 354–359, 2017.
- [3] C. Berner, G. Brockman, B. Chan, V. Cheung, P. Debiak, C. Dennison, D. Farhi, Q. Fischer, S. Hashme, C. Hesse et al., "Dota 2 with large scale deep reinforcement learning," *arXiv preprint arXiv:1912.06680*, 2019.
- [4] S. Gu, E. Holly, T. Lillicrap, and S. Levine, "Deep reinforcement learning for robotic manipulation with asynchronous off-policy updates," in *2017 IEEE international conference on robotics and automation (ICRA)*. IEEE, 2017, pp. 3389–3396.
- [5] D. Kalashnikov, A. Irpan, P. Pastor, J. Ibarz, A. Herzog, E. Jang, D. Quillen, E. Holly, M. Kalakrishnan, V. Vanhoucke et al., "Scalable deep reinforcement learning for vision-based robotic manipulation," in *Conference on Robot Learning*. PMLR, 2018, pp. 651–673.
- [6] X. B. Peng, M. Andrychowicz, W. Zaremba, and P. Abbeel, "Sim-to-real transfer of robotic control with dynamics randomization," in *2018 IEEE international conference on robotics and automation (ICRA)*. IEEE, 2018, pp. 3803–3810.
- [7] T. P. Lillicrap, J. J. Hunt, A. Pritzel, N. Heess, T. Erez, Y. Tassa, D. Silver, and D. Wierstra, "Continuous control with deep reinforcement learning," *arXiv preprint arXiv:1509.02971*, 2015.
- [8] O. M. Andrychowicz, B. Baker, M. Chociej, R. Jozefowicz, B. McGrew, J. Pachocki, A. Petron, M. Plappert, G. Powell, A. Ray et al., "Learning dexterous in-hand manipulation," *The International Journal of Robotics Research*, vol. 39, no. 1, pp. 3–20, 2020.
- [9] J. Schulman, F. Wolski, P. Dhariwal, A. Radford, and O. Klimov, "Proximal policy optimization algorithms," *arXiv preprint arXiv:1707.06347*, 2017.
- [10] J. Schulman, S. Levine, P. Abbeel, M. Jordan, and P. Moritz, "Trust region policy optimization," in *Proceedings of The 32nd International Conference on Machine Learning*, 2015, pp. 1889–1897.
- [11] S. Fujimoto, H. Hoof, and D. Meger, "Addressing function approximation error in actor-critic methods," in *International Conference on Machine Learning*. PMLR, 2018, pp. 1587–1596.
- [12] T. Haarnoja, A. Zhou, P. Abbeel, and S. Levine, "Soft actor-critic: Off-policy maximum entropy deep reinforcement learning with a stochastic actor," in *International Conference on Machine Learning*. PMLR, 2018, pp. 1861–1870.
- [13] G. Brockman, V. Cheung, L. Pettersson, J. Schneider, J. Schulman, J. Tang, and W. Zaremba, "Openai gym," *arXiv preprint arXiv:1606.01540*, 2016.
- [14] R. Mahjourian, R. Miikkulainen, N. Lazic, S. Levine, and N. Jaitly, "Hierarchical policy design for sample-efficient learning of robot table tennis through self-play," *arXiv preprint arXiv:1811.12927*, 2018.
- [15] O. Koç, G. Maeda, and J. Peters, "Online optimal trajectory generation for robot table tennis," *Robotics and Autonomous Systems*, vol. 105, pp. 121–137, 2018.
- [16] R. Silva, F. S. Melo, and M. Veloso, "Towards table tennis with a quadrotor autonomous learning robot and onboard vision," in *2015 IEEE/RSJ International Conference on Intelligent Robots and Systems (IROS)*. IEEE, 2015, pp. 649–655.
- [17] D. Büchler, S. Guist, R. Calandra, V. Berenz, B. Schölkopf, and J. Peters, "Learning to play table tennis from scratch using muscular robots," *arXiv preprint arXiv:2006.05935*, 2020.
- [18] P. Blank, B. H. Groh, and B. M. Eskofier, "Ball speed and spin estimation in table tennis using a racket-mounted inertial sensor," in *Proceedings of the 2017 ACM International Symposium on Wearable Computers*, 2017, pp. 2–9.
- [19] J. Tebbe, L. Klamt, Y. Gao, and A. Zell, "Spin detection in robotic table tennis," in *2020 IEEE International Conference on Robotics and Automation (ICRA)*. IEEE, 2020, pp. 9694–9700.
- [20] W. Gao, L. Graesser, K. Choromanski, X. Song, N. Lazic, P. Sanketi, V. Sindhwani, and N. Jaitly, "Robotic table tennis with model-free reinforcement learning," *arXiv preprint arXiv:2003.14398*, 2020.
- [21] Y. Zhu, Y. Zhao, L. Jin, J. Wu, and R. Xiong, "Towards high level skill learning: Learn to return table tennis ball using monte-carlo based policy gradient method," in *2018 IEEE International Conference on Real-time Computing and Robotics (RCAR)*. IEEE, 2018, pp. 34–41.
- [22] J. Tebbe, L. Krauch, Y. Gao, and A. Zell, "Sample-efficient reinforcement learning in robotic table tennis," *arXiv preprint arXiv:2011.03275*, 2020.
- [23] J. Tebbe, Y. Gao, M. Sastre-Rienietz, and A. Zell, "A table tennis robot system using an industrial kuka robot arm," in *German Conference on Pattern Recognition*. Springer, 2018, pp. 33–45.
- [24] Y. Zhang, Y. Zhao, R. Xiong, Y. Wang, J. Wang, and J. Chu, "Spin observation and trajectory prediction of a ping-pong ball," in *2014 IEEE International Conference on Robotics and Automation (ICRA)*. IEEE, 2014, pp. 4108–4114.
- [25] P. Blank, B. H. Groh, and B. M. Eskofier, "Ball speed and spin estimation in table tennis using a racket-mounted inertial sensor," in *Proceedings of the 2017 ACM International Symposium on Wearable Computers*, 2017, pp. 2–9.
- [26] T. Xu, Q. Liu, L. Zhao, and J. Peng, "Learning to explore via meta-policy gradient," in *International Conference on Machine Learning*. PMLR, 2018, pp. 5463–5472.
- [27] T. Kröger, *On-Line Trajectory Generation in Robotic Systems: Basic Concepts for Instantaneous Reactions to Unforeseen (Sensor) Events*. Springer, 2010, vol. 58.
- [28] K. Mülling, J. Kober, O. Kroemer, and J. Peters, "Learning to select and striking movements in robot table tennis," *The International Journal of Robotics Research*, vol. 32, no. 3, pp. 263–279, 2013.
- [29] K. ASAI, M. Nakayama, and S. YASE, "The ping pong robot to return a ball precisely," Nov. 2019. [Online]. Available: <https://www.omron.com/global/en/technology/omrontechnics/vol51/016.html>